# Four copper(II) pyrazolido complexes derived from reactions of 3{5}-substituted pyrazoles with $CuF_2$ or $Cu(OH)_2$†‡

**Q. Folshade Mokuolu,[a] Dolos Foguet-Albiol,[b] Leigh F. Jones,[a] Joanna Wolowska,[c] Radoslaw M. Kowalczyk,[c] Colin A. Kilner,[a] George Christou,[b] Patrick C. McGowan[a] and Malcolm A. Halcrow*[a]**

***Received 2nd January 2007, Accepted 20th February 2007***
***First published as an Advance Article on the web 9th March 2007***
**DOI: 10.1039/b618780c**

Treatment of $CuF_2$ with 2 equiv of 3{5}-[pyrid-2-yl]pyrazole ($Hpz^{Py}$), 3{5}-phenylpyrazole ($Hpz^{Ph}$) or 3{5}-[4-fluorophenyl]pyrazole ($Hpz^{PhF}$) in MeOH, followed by evaporation to dryness and recrystallisation of the solid residues, allows solvated crystals of $[\{Cu(\mu\text{-}pz^{Py})(pz^{Py})\}_2]$ (**1**), $[\{Cu(\mu\text{-}pz^{Ph})_2\}_4]$ (**2**) and $[Cu_4F_2(\mu_4\text{-}F)(\mu\text{-}pz^{PhF})_5(Hpz^{PhF})_4]$ (**3**) to be isolated in moderate-to-good yields. Similar reactions of these three pyrazoles with $Cu(OH)_2$ in refluxing MeOH respectively afford **1**, **2** and $[Cu(pz^{PhF})_2(Hpz^{PhF})_2]$ (**4**) in *ca.* 10% yield. Crystalline $\mathbf{1}\cdot 1/2H_2O\cdot 2CHCl_3$ contains two independent dinuclear molecules with a puckered di-(1,2-pyrazolido) bridge motif, linked by a bridging, hydrogen-bonding water molecule. Compound $\mathbf{2}\cdot 1/2C_5H_{12}$, containing cyclic, square tetranuclear complex molecules, is the first homoleptic divalent metal pyrazolide to have a discrete molecular rather than polymeric structure, for a metal other than Pd or Pt. The two independent complex molecules in $\mathbf{3}\cdot 3/4CH_2Cl_2\cdot Hpz^{PhF}$ contain a unique tetrahedral $[Cu_4(\mu_4\text{-}F)]^{7+}$ core, three of whose edges are spanned by bridging pyrazolido groups. Magnetic data show that the copper centres in **1** and **3** are antiferromagnetically coupled, but that dried bulk samples of **2** do not retain their molecular structure.

## Introduction

Pyrazoles are very versatile bridging ligands in transition metal chemistry. When deprotonated, they can link two metal ions through their two adjacent N donors, which typically places the metal ions 3.5–4.5 Å apart. A wide variety of dinuclear and polynuclear organometallic and coordination complexes have been prepared containing 1,2-pyrazolido bridges,[1] including organometallic catalysts,[1,2] cyclic toroidal host : guest complexes[1,3] and other high-nuclearity structures.[1,4] Conversely, in their neutral form, pyrazoles can bond simultaneously to metal ions (through their pyridinic N atom) and to anions (by donating hydrogen bonds with their pyrrolic N–H groups), making pyrazoles useful ditopic ligands for metal salts.[5–8] While metal pyrazole complex chemistry is very well established, we have found that addition of base to reactions of copper salts with simple pyrazoles can lead to novel polymetallic structures, containing both types of bridging pyrazole ligand.[9–12] Of particular relevance here is the cyclic hexanuclear compound $[\{Cu_3(Hpz^{tBu})_4(\mu\text{-}pz^{tBu})_2(\mu\text{-}F)_2(\mu_3\text{-}F)\}_2]F_2$, formed in good yield from the reaction of $CuF_2$, 3{5}-*tert*butylpyrazole ($Hpz^{tBu}$) and NaOH in MeOH, which contains two encapsulated fluoride ions within tris-pyrazole pockets on opposite sides of the molecule.[10,11] We were keen to examine reactions of other pyrazole derivatives with $CuF_2$, to see if other similarly novel structures could be prepared. We report here three very different copper(II) complexes obtained in this way. One of these is a homoleptic copper(II) pyrazolide with a unique molecular, rather than polymeric,[13] structure, while another is a tetranuclear complex with a novel fluoro-centred tetrahedral metal core.

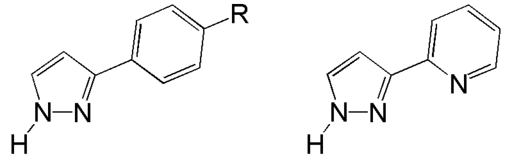

R = H, $Hpz^{Ph}$
R = F, $Hpz^{PhF}$

$Hpz^{Py}$

## Results and discussion

Treatment of $CuF_2$ with two molar equiv. of 3{5}-(pyrid-2-yl)pyrazole ($Hpz^{Py}$)[14] in MeOH at room temperature, in the presence of two equiv. of NaOH, yields a blue solution. This was filtered, evaporated to dryness and the solid residue extracted into chloroform. Addition of a large excess of pentane to the resultant solution and storage at −30 °C, led to the slow formation of blue crystals that were formulated as $[\{Cu(\mu\text{-}pz^{Py})(pz^{Py})\}_2]\cdot 1/2H_2O\cdot 2CHCl_3$ ($\mathbf{1}\cdot 1/2H_2O\cdot 2CHCl_3$) by a crystal structure determination. An analogous reaction employing 3{5}-phenylpyrazole ($Hpz^{Ph}$)[15] afforded the dark green hemipentane solvate of the tetranuclear product $[\{Cu(\mu\text{-}pz^{Ph})_2\}_4]$ ($\mathbf{2}\cdot 1/2C_5H_{12}$). Interestingly, however, a very similar procedure

---

[a] *School of Chemistry, University of Leeds, Woodhouse Lane, Leeds, UK LS2 9JT. E-mail: m.a.halcrow@ leeds.ac.uk*
[b] *Department of Chemistry, University of Florida, P.O. Box 117200, Gainesville, FL, 32611-7200, USA*
[c] *Department of Chemistry, University of Manchester, Oxford Road, Manchester, UK M13 9PL*
† The HTML version of this article has been enhanced with colour images.
‡ Electronic supplementary information (ESI) available: Figures and Tables of metric parameters for the crystal structures in this work, and Figures showing magnetic data for **2** and the X-band EPR spectra of **1** and **3**. See DOI: 10.1039/b618780c

with 3{5}-(4-fluorophenyl)pyrazole (Hpz$^{PhF}$)[16] and excess triethylamine as base, afforded blue–green crystals of a third, very different tetranuclear product of formula [$Cu_4F_2(\mu_4$-F)(μ-Pz$^{PhF}$)$_5$(HPz$^{PhF}$)$_4$]·3/4CH$_2$Cl$_2$·HPz$^{PhF}$ (**3**·3/4CH$_2$Cl$_2$·Hpz$^{PhF}$). All these compounds were obtained in moderate yields, ranging from 30–68%. Reactions of Hpz$^{Py}$ and Hpz$^{Ph}$ with Cu(OH)$_2$ in refluxing MeOH again afforded **1** and **2**, albeit in much lower yields of *ca.* 10% reflecting the insolubility of the Cu(OH)$_2$ starting material. However, the only crystalline product obtained from reactions of HPz$^{PhF}$ with Cu(OH)$_2$ was instead mononuclear [Cu(pz$^{PhF}$)$_2$(Hpz$^{PhF}$)$_2$] (**4**), which formed blue solvent-free crystals in 13% yield from CH$_2$Cl$_2$/Et$_2$O (ESI‡). The solvated crystals of **1–3** all collapsed upon drying *in vacuo* to powdered solids, whose microanalyses were consistent with the formulations of the unsolvated complexes. All magnetochemical and spectroscopic measurements were performed using these dried powders.

The asymmetric unit of **1**·1/2H$_2$O·2CHCl$_3$ contains two unique complex molecules (labelled "A" and "B") linked by a bridging hydrogen-bonded water molecule, and four molecules of chloroform, two of which also donate hydrogen bonds (Fig. 1). The two complex molecules have identical connectivities, being dimers of five-coordinate metal ions with apical pyridyl donors (Fig. 1, ESI‡). The molecules differ, however, in that the copper ions in molecule A show stronger distortions away from an ideal square-pyramidal geometry than in molecule B. That is evident in their $\tau$ values, which are 0.438(3) [for Cu(1A)], 0.454(3) [Cu(2A)], 0.311(3) [Cu(1B)] and 0.253(3) [Cu(2B)] ($\tau = 0$ and 1 for ideal square pyramidal and trigonal bipyramidal stereochemistries, respectively[17]). The more regular geometry of molecule B is also reflected in its apical bond lengths Cu(1B)–N(31B) and Cu(2B)–N(42B), which are 0.048(4)–0.063(4) Å longer than the corresponding bonds in molecule A (ESI‡). The apical pyridyl groups C(30)–C(35) and C(41)–C(46) in the two molecules are *syn* to each other across their [Cu$_2$(μ-pz$^{Py}$)$_2$]$^{2+}$ bridges, being 3.2–3.4 Å apart at their closest approach. However, the large dihedral angles between these moieties [32.25(19)° in molecule A and 35.99(17)° in molecule B], which are a consequence of the puckered [Cu$_2$(μ-pz$^{Py}$)$_2$]$^{2+}$ geometry, means that these pyridyl rings do not form $\pi$–$\pi$ interactions with each other. Three of the four uncoordinated pyrazolido N atoms in the two structures accept intermolecular hydrogen bonds. These are two O–H···N interactions, from water molecule O(63) to N(37A) and N(26B); and a C–H···N bond from chloroform molecule C(59)–Cl(62) to N(37B). There is also one further C–H···O interaction from another chloroform molecule C(47)–Cl(50) to O(63).

While the crystallographic data and refinement are good, the structure determination of **2**·1/2C$_5$H$_{12}$ is complicated by disorder in both the solvent and three of the [pz$^{Ph}$]$^-$ ligands. The structure analysis showed that **2** has a cyclic tetrameric structure, with four four-coordinate Cu ions each linked to its neighbours by two [pz$^{Ph}$]$^-$ bridges (Fig. 2, ESI‡). The molecule has approximate $S_4$ symmetry, although there are several local structural distortions away from this idealised symmetry. Each of the four Cu$_2$(μ-pz$^{Ph}$)$_2$ moieties in the compound has a head-to-head disposition of phenyl groups, presumably to avoid steric clashes between them. The coordination geometry at the four Cu centres shows a substantial tetrahedral twist. The crystallographically ordered *trans*-N–Cu–N angles in the structure range from 142.78(9)–154.97(9)°, while the dihedral angle between the planes [Cu(3), N(49), N(60)] and [Cu(3), N(49), N(60)] is 43.97(9)° (Cu(3) is the only Cu atom in the structure bound to four crystallographically ordered N-donors). This geometry is similar to that adopted by other copper(II) di(pyrazolide) salts, which adopt 1-D polymeric

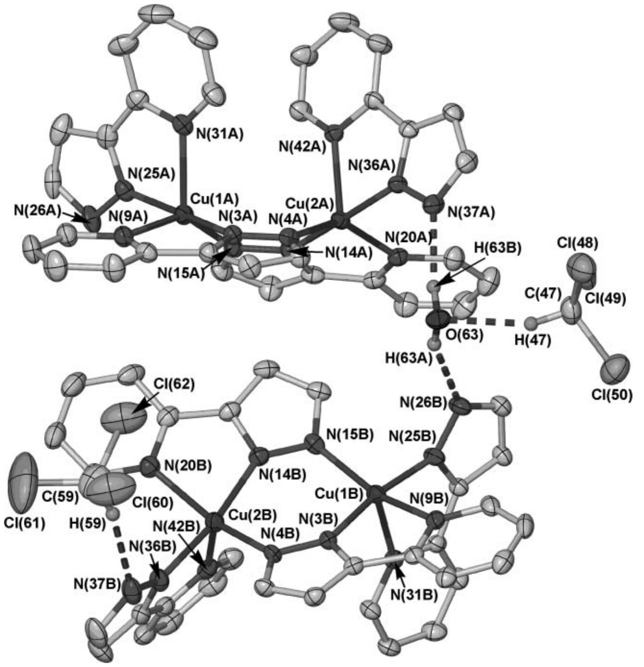

**Fig. 1** View of the formula unit in the crystal structure of **1**·1/2H$_2$O·2CHCl$_3$. For clarity, all H atoms not involved in hydrogen-bonding have been omitted, while the two CHCl$_3$ molecules that do not donate hydrogen bonds are not shown. Thermal ellipsoids are at the 50% probability level.

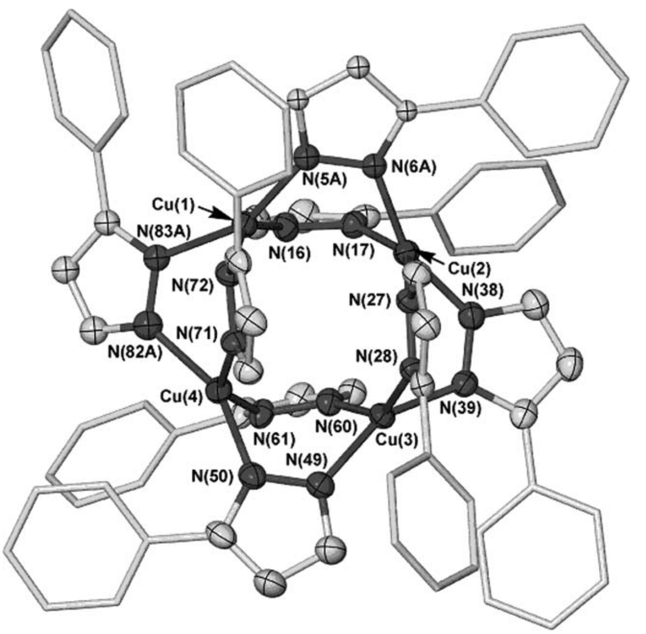

**Fig. 2** View of the complex molecule in the crystal structure of **2**·1/2C$_5$H$_{12}$. For clarity, only one orientation of the disordered pyrazolide ligands and phenyl group is shown, while all H atoms have been omitted. Thermal ellipsoids are at the 50% probability level except for the phenyl substituents which have arbitrary radii.

structures with *trans*-N–Cu–N angles of 139.5(1)–140.8(3)°.[13] The Cu–N bond lengths in **2** are typical for four-coordinate copper(II) centres, while the Cu···Cu distances between directly linked Cu ions lie between 3.2771(7)–3.3342(7) Å. Space-filling models of **2** show that there is no cavity within the cyclic molecule.

Crystals of **3**·3/4$CH_2Cl_2$·$Hpz^{PhF}$ again contain two independent complex molecules labelled "A" and "B", with identical connectivities, similar patterns of pyrazole ligand disorder (see Experimental section) and only small differences in their metric parameters (ESI‡). The four copper ions in **3** are disposed in a distorted tetrahedral arrangement, that is approximately $C_2$-symmetric if the aryl substituents on the pyrazole groups are ignored. This copper tetrahedron is centred by a $\mu_4$-$F^-$ ion, forming four Cu–F bonds of 2.226(2)–2.324(2) Å (Fig. 3 and 4, ESI‡). Two opposite edges of the copper tetrahedra are bridged by two μ-1,2-$[Pz^{PhF}]^-$ ligands, one pair having a head-to-head disposition of phenyl substituents and the other being head-to-tail. A third edge bears a single μ-1,2-$[Pz^{PhF}]^-$ bridging ligand, while the other three edges are unbridged. The eight individual copper ions in the asymmetric unit all have geometries that are close to square pyramidal with F(1A) or F(1B) apical, with $\tau = 0.164(3)$–$0.321(3)$.[17] The basal planes of Cu(1) and Cu(2) in each molecule are formed by two *cis* μ-$[Pz^{PhF}]^-$ ligands, and by terminal $F^-$ and terminal $HPz^{PhF}$ ligands, while those of Cu(3) and Cu(4) are bound by three μ-$[Pz^{PhF}]^-$ and one terminal $HPz^{PhF}$ ligands. Each terminal fluoride ligand accepts N–H···F hydrogen bonds from two of the four $HPz^{PhF}$ moieties in the molecules. The geometry at $\mu_4$-$F^-$ ligand F(1X) (X = A or B) is somewhat flattened, since two opposite edges of the $[Cu_4(\mu_4\text{-}F)]^{7+}$ tetrahedron are spanned by very obtuse angles [Cu(1X)–F(1X)–Cu(3X) and Cu(2X)–F(1X)–Cu(4X)] of 133.68(9)–137.55(10)°, while three of the other four Cu–F(1X)–Cu angles in each molecule have contracted to 89.06(7)–93.10(8)° to compensate. However, the average of the six Cu–F(1X)–Cu angles in molecules A and B is 110.1(2) and 110.4(2)° respectively, showing that this geometry is best considered as distorted tetrahedral.

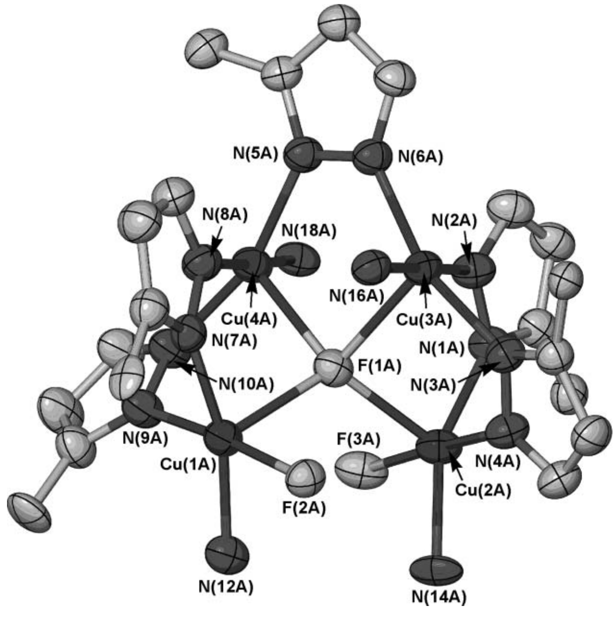

**Fig. 3** View of the core of complex molecule 'A' in **3**·3/4$CH_2Cl_2$·$Hpz^{PhF}$, showing the atom numbering scheme employed. Only the coordinated N atoms of the $Hpz^{PhF}$ ligands, and only the *ipso* phenyl C atoms of the $[pz^{PhF}]^-$ ligands, are shown. Molecule 'B' is visually almost identical to molecule A and uses an identical atom numbering with 'B' label suffixes. Thermal ellipsoids are at the 50% probability level.

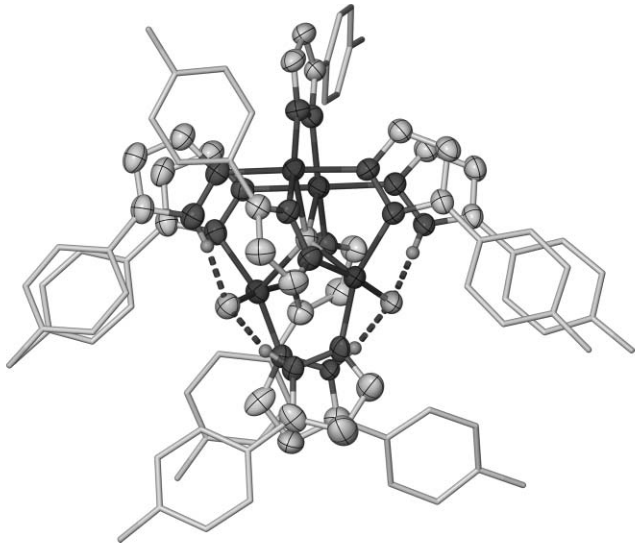

**Fig. 4** View of the complete molecule 'B' in **3**·3/4$CH_2Cl_2$·$Hpz^{PhF}$. For clarity only one orientation of the disordered $[pz^{PhF}]^-$ ligands is shown, and all C-bound H atoms have been omitted. Thermal ellipsoids are at the 50% probability level except for H atoms and the 4-fluorophenyl substituents, which have arbitrary radii. Other details as for Fig. 3.

Crystals of **4** contain discrete, mononuclear $[Cu(pz^{PhF})_2(Hpz^{PhF})_2]$ molecules, whose square-planar geometry has a significant tetrahedral twist with *trans*-N–Cu–N angles of 140.69(16)–143.76(16)° (ESI‡). The protonated and deprotonated pyrazole ligands are crystallographically distinguishable (see Experimental section), and form two intramolecular N–H···N hydrogen bonded pairs.

At room temperature $\chi_M T$ for **1** is 0.7 $cm^3\ mol^{-1}$ K, slightly smaller than the value expected from two independent copper(II) ions with a sensible *g* value (*ca.* 0.8 $cm^3\ mol^{-1}$ K[18]). As the temperature is decreased $\chi_M T$ also decreases steadily, reaching 0.05 $cm^3\ mol^{-1}$ K at 45 K and then continuing to decrease more slowly as the temperature is lowered further. These data were well-reproduced by the Bleaney–Bowers equation for a dicopper(II) complex ($H = -2J(S_1 \cdot S_2)$ Hamiltonian),[18] giving $J = -88.7(5)\ cm^{-1}$, $g = 2.13(1)$ and a paramagnetic impurity term $\rho = 7.8(2)\%$. The refined value of *g* agrees well with the average *g* value predicted by the solid-state EPR spectrum of **1**, $g_{iso} = 2.12$ (see below).

The variable temperature susceptibility data for **3** are similar in form to those of **1**, decreasing steadily from $\chi_M T = 1.4\ cm^3\ mol^{-1}$ K at 330 K to 0.10 $cm^3\ mol^{-1}$ K at 40 K before decreasing more slowly as the temperature is lowered to 5 K (Fig. 5). These data were modelled using the Hamiltonian in eqn (1):

$$H = -2J_1(S_1 \cdot S_4 + S_2 \cdot S_3) - 2J_2(S_3 \cdot S_4) \qquad (1)$$

where $S_1$–$S_4$ correspond to the equivalently numbered Cu atoms in the crystal structure of **3** ($S_1 \equiv$ Cu(1) *etc.*, Fig. 3). Hence, $J_1$ describes superexchange across the two $[Cu_2(\mu\text{-}pz^{PhF})_2(\mu\text{-}F)]^+$ bridging groups, while $J_2$ describes superexchange mediated by the $[Cu_2(\mu\text{-}pz^{Ph})(\mu\text{-}F)]^{2+}$ moiety in the structure. Magnetic coupling between Cu(1) and Cu(2), Cu(1) and Cu(3), and Cu(2) and Cu(4),

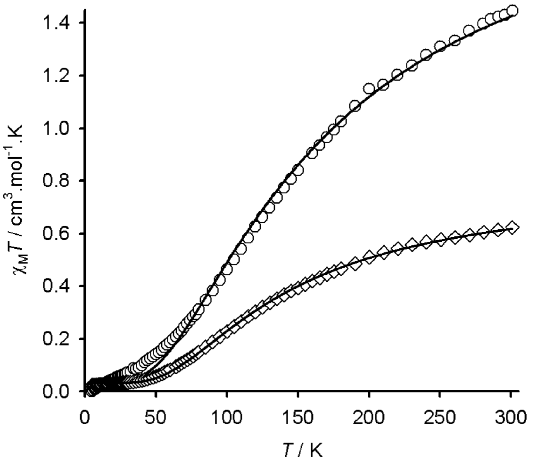

**Fig. 5** Variable temperature magnetic susceptibility data for **1** (◇) and **3** (○), and the best fits of these data (lines) to the equations described in the text. Data for **2** are given in the ESI‡.

is expected to be weak because these pairs of copper ions are only covalently bridged by the apical $\mu_4$-F$^-$ ligand, which does not interact directly with their $d_{xy}$ magnetic orbitals. Hence, to avoid over-parametrisation these interactions were neglected in the magnetochemical analysis. The spin-energy levels described by eqn (1) have been elucidated by others[19] and the susceptibility data for **3** were reproduced reasonably by the resultant van Vleck equation (Fig. 5), giving the parameters $J_1 = -97.9(7)$ cm$^{-1}$, $J_2 = -68(5)$ cm$^{-1}$ and $\rho = 10(1)\%$. Attempts to refine the $g$ term in these fits led to strongly correlated $g$ and $J$ values. Hence $g$ was fixed at 2.14, the value derived by EPR (see below), in the final fit. The small deviation of the simulation from the observed data below 50 K, and the slightly high value of $\rho$ (which is also governed by the low-temperature data), may reflect the approximations in the model used which neglects any weak superexchange mediated by the apical F$^-$ ligand.

The values of $J$ for **1** and $J_1$ for **3** derived from these analyses are typical values for copper centres linked by bis- pyrazolido bridges, for which $-240 \leq J \leq -70$ cm$^{-1}$ is typically observed.[20–22] The value of $J_2$ for **3** is higher than usually found in dinuclear copper(II) complexes with a single pyrazolido bridge, which lie in the range $-32 \leq J \leq -12$ cm$^{-1}$.[20,23,24] However, a similar $J$ value ($J \approx -78$ cm$^{-1}$) has been proposed for one other tetranuclear copper(II) complex containing mono-pyrazolido bridging groups.[24]

In contrast to **1** and **3**, magnetic data for **2** were sample-dependent. A typical measurement showed an almost monotonic decrease in $\chi_M T$ with temperature, from 1.5–1.7 cm$^3$ mol$^{-1}$ K at room temperature to near-zero at 5 K (ESI‡). This linear temperature dependence cannot be reproduced by the Hamiltonian describing a square of copper(II) spins (eqn (2)):

$$H = -2J_1(S_1 \cdot S_2 + S_2 \cdot S_3 + S_3 \cdot S_4 + S_4 \cdot S_1) \qquad (2)$$

which predicts a $\chi_M T$ *vs.* $T$ curve of similar shape to that shown by **3** (ESI‡). Attempts to model the data as a 1-D polymer of copper(II) spins, the structure adopted by other homoleptic copper(II) pyrazolides,[13] were similarly unsuccessful. These data imply that, despite their apparent analytical purity, bulk samples of **2** do not contain purely the tetrameric molecule observed in the solvated crystals and are probably inhomogeneous.

The $X$-band (9.35 GHz) EPR spectrum of powdered **1** at 115 K is typical of a $S = 1$ spin-system, and shows a pronounced $\Delta m_s = \pm 2$ half-field resonance near 1590 G (ESI‡). This spectrum was further resolved at $W$-band (94.0 GHz) at 100 K, into a clearly rhombic spectrum with the six resonance lines expected from a randomly oriented rhombic spin–triplet (Fig. 6). Because of the low probability of the formally forbidden "half-field" transition at higher magnetic fields no such signal was observed at $W$-band.

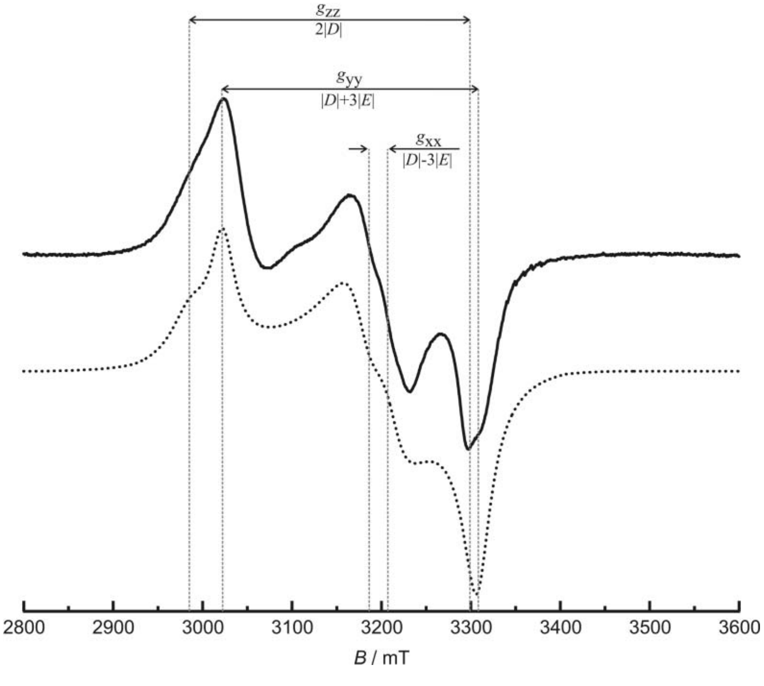

**Fig. 6** Observed (top) and simulated (bottom) $W$-band EPR spectrum of solid **1** at 100 K. Parameters derived from the simulation are given in the text.

From a simulation the following data were extracted: $g_{xx} = 2.100(1)$, $g_{yy} = 2.121(1)$ $g_{zz} = 2.135(1)$, $|D| = 0.158(2)$ cm$^{-1}$ and $|E| = 0.041(2)$ cm$^{-1}$ (Fig. 6). The value of $|D|$ suggests only a limited level of delocalisation of the unpaired electron density, whereas $|E|$ reflects significant distortion of the spectrum from the axial symmetry ($3|E|/|D| = 0.78$). The EPR spectra of solid **2** and **3** are less informative, showing single isotropic lines at $g = 2.12$ (**2**) and 2.14 (**3**) at *X*-band at 115 K. Compound **3** (but not **2**) also exhibits a weak half-field resonance under these conditions, consistent with its being an integer-spin system.

## Conclusions

There are three other dicopper(II) complexes comparable to **1** in the literature.[8,20,25] Of particular relevance is $[Cu_2(\mu\text{-}pz^{Py})_2(Hpz^{Py})_2][ClO_4]_2$, the doubly protonated congener of **1** ([**1**$H_2$][$ClO_4$]$_2$)[25] While the basic connectivity in **1** and [**1**$H_2$][$ClO_4$]$_2$ is the same, they differ in that [**1**$H_2$][$ClO_4$]$_2$ crystallises with *anti* rather than *syn* apical pyridyl groups and has a perfectly planar $[Cu_2(\mu\text{-}pz^{Py})_2]^{2+}$ bridge motif. Several different magnetostructural correlations have been proposed for $[Cu_2(\mu\text{-pyrazolido})_2]^{2+}$ complexes,[22,26] making it difficult to rationalise simply the weaker antiferromagnetism of **1** [$J = -88.7(5)$ cm$^{-1}$] compared to [**1**$H_2$][$ClO_4$]$_2$ [$-105$ cm$^{-1}$].[25] However, the puckered $[Cu_2(\mu\text{-}pz^{Py})_2]^{2+}$ group in **1** is probably a contributing factor, since it has been shown that $J$ is reduced if the two bridging pyrazolido groups in these compounds are not coplanar.[26]

Although we only achieved limited characterisation of bulk samples of **2**, which apparently decompose upon exposure to air, its molecular structure is of some interest. First, **2** is notable as the first homoleptic divalent metal pyrazolide to have a discrete molecular rather than a 1-D polymeric structure,[13,27] for a metal other than Pd or Pt.[28–30] Second, the tetranuclear structure of **2** contrasts with the corresponding palladium(II) complex $[\{Pd(\mu\text{-}pz^{Ph})_2\}_3]$[28] which, like nearly all known palladium(II) and platinum(II) pyrazolides,[28–30] adopts a cyclic *trinuclear* structure containing near-regular square-planar palladium(II) centres. The increased nuclearity of **2** compared to the Pd compound cannot reflect the different radii of their respective metals, since the Cu–N and Pd–N bond lengths in the two compounds are essentially identical. Rather, we tentatively suggest that it may be a consequence of the increased tetrahedral distortion of the ligand donors about Cu in **2**, compared to the near-regular planar stereochemistry at Pd. Since the tetrahedrally distorted Cu geometry in **2** is also common to other, polymeric copper(II) pyrazolides,[13] that would imply that the structure of **2** is dictated by the structural preferences of copper(II) tetrakis-pyrazolido centres, rather than by the steric properties of the $[pz^{Ph}]^-$ phenyl substituents. Similar structural comparisons can also be made with **4**, which adopts a very similar tetrahedrally twisted geometry with intramolecular N–H · · · N hydrogen bonding. This contrasts with $[Pd(pz^*)_2(Hpz^*)_2]$ (Hpz* = 3,5-dimethylpyrazole)[31] and $[Pt(pz)_2(Hpz)_2]$ (Hpz = pyrazole),[32] which have more regular square-planar stereochemistries and associate into dimers through intermolecular N–H · · · N hydrogen bonds.

Only five other transition metal complexes containing a $\mu_4$-F$^-$ ligand, as in **3**, have been crystallographically characterised, all of which contain d$^0$ molybdenum(VI),[33] vanadium(V)[34] or titanium(IV)[35] metal ions. A small number of other $\mu_4$-F$^-$ compounds are also known that contain group 1 or group 2 metals,[36] or a lanthanide ion.[37] Hence, **3** is unique as a $\mu_4$-F$^-$ complex containing a late transition ion in a moderate oxidation state. As in most (but not all[31]) of these other examples the $\mu_4$-F$^-$ in **3** is in an approximately tetrahedral environment.

## Experimental

Ligands $Hpz^{Py}$,[14] $Hpz^{Ph}$[15] and $Hpz^{PhF}$[16] were synthesised according to the literature procedures. All other reagents and AR-grade solvents were purchased commercially and used as supplied.

### Synthesis of $[\{Cu(\mu\text{-}pz^{Py})(pz^{Py})\}_2]$ (1)

Addition of $Hpz^{Py}$ (0.61 g, 4.2 mmol) to a solution of $CuF_2$ (0.21 g, 2.1 mmol), and NaOH (0.17 g, 4.2 mmol) in MeOH (50 cm$^3$) yielded an immediate blue precipitate, which dissolved upon stirring at room temperature for 2 h. The resultant dark blue solution was filtered and evaporated to dryness, and the solid residues extracted with the minimum volume of $CHCl_3$. Layering the filtered solution with a five-fold excess of pentane resulted in the formation of blue crystals over a period of days. These were collected, washed with pentane and dried *in vacuo.* Yield 0.36 g, 49%. Found C, 55.2; H, 4.1; N, 23.0%. Calcd for $C_{32}H_{24}Cu_2N_{12}$ C, 54.6; H, 3.4; N, 23.9%. FD mass spectrum ($CHCl_3$): *m/z* 1467 $[^{63}Cu_5(pz^{Py})_8]^+$, 1323 $[^{63}Cu_5(pz^{Py})_7]^+$, 1260 $[^{63}Cu_4(pz^{Py})_7]^+$, 1242 $[^{63}Cu_6(pz^{Py})_6]^+$, 1179 $[^{63}Cu_5(pz^{Py})_6]^+$, 1116 $[^{63}Cu_4(pz^{Py})_6]^+$, 1035 $[^{63}Cu_5(pz^{Py})_5]^+$, 972 $[^{63}Cu_4(pz^{Py})_5]^+$, 765 $[^{63}Cu_3(pz^{Py})_4]^+$, 704 $[^{63}Cu_2(pz^{Py})_2(Hpz^{Py})_2]^+$, 622 $[^{63}Cu_3(pz^{Py})_3]^+$, 558 $[^{63}Cu_2(pz^{Py})_3]^+$, 414 $[^{63}Cu_2(pz^{Py})_2]^+$, 351 $[^{63}Cu(pz^{Py})_2]^+$, 145 $[Hpz^{Py}]^+$. ES mass spectrum (MeCN): *m/z* 765 $[^{63}Cu_3(pz^{Py})_4]^+$, 665 $[^{63}Cu_3(Hpz^{Py})_3(CH_3CN)]^+$, 558 $[^{63}Cu_2(pz^{Py})_3]^+$, 455 $[^{63}Cu_2(pz^{Py})_2(CH_3CN)]^+$, 414 $[^{63}Cu_2(pz^{Py})_2]^+$, 351 $[\{^{63}Cu(pz^{Py})_2\}_x]^{x+}$ ($x = 1$ or 2), 248 $[\{^{63}Cu(pz^{Py})(CH_3CN)\}_x]^{x+}$ ($x = 1$ or 2), 207 $[\{^{63}Cu(pz^{Py})\}_x]^{x+}$ ($x = 1$ or 2), 146 $[H_2pz^{Py}]^+$.

### Synthesis of $[\{Cu(\mu\text{-}pz^{Ph})_2\}_4]$ (2)

A mixture of $CuF_2$ (0.21 g, 2.1 mmol), $Hpz^{Ph}$ (0.60 g, 4.2 mmol) and NaOH (0.17 g, 4.2 mmol) in MeOH (50 cm$^3$) was stirred at room temperature for 3 days, yielding a dark green solution. The mixture was then evaporated to dryness, and the solid residues extracted with the minimum volume of $CH_2Cl_2$. Layering the filtered solution with a five-fold excess of pentane resulted in the formation of dark green crystals over a period of days. These were collected, washed with pentane and dried *in vacuo.* Yield 0.50 g, 68%. Found C, 61.9; H, 3.9; N, 16.3%. Calcd for $C_{72}H_{56}Cu_4N_{16}$ C, 62.4; H, 4.0; N, 15.7%. FD mass spectrum ($CHCl_3$): *m/z* 1110 $[^{63}Cu_4(pz^{Ph})_6]^+$, 1047 $[^{63}Cu_3(pz^{Ph})_6]^+$, 904 $[^{63}Cu_3(pz^{Ph})_5]^+$, 761 $[^{63}Cu_3(pz^{Ph})_4]^+$, 618 $[^{63}Cu_3(pz^{Ph})_3]^+$, 144 $[Hpz^{Ph}]^+$. ES mass spectrum (MeCN): *m/z* 555 $[^{63}Cu_2(pz^{Ph})_3]^+$, 455 $[\{^{63}Cu_2(pz^{Ph})_2(CH_3CN)\}_x]^{x+}$ ($x = 1$ or 2), 414 $[^{63}Cu_2(pz^{Ph})_2]^+$, 413 $[\{^{63}Cu_2(pz^{Ph})(Hpz^{Ph})\}_x]^{x+}$ ($x = 1$ or 2), 350 $[\{^{63}Cu(pz^{Ph})(Hpz^{Ph})\}_x]^{x+}$ ($x = 1$ or 2), 247 $[\{^{63}Cu(pz^{Ph})(CH_3CN)\}_x]^{x+}$ ($x = 1$ or 2), 145 $[H_2pz^{Ph}]^+$.

### Synthesis of $[Cu_4F_2(\mu_4\text{-}F)(\mu\text{-}pz^{PhF})_5(Hpz^{PhF})_4]$ (3)

Reaction of $CuF_2$ (0.21 g, 2.1 mmol), $Hpz^{PhF}$ (0.68 g, 4.2 mmol) and $NEt_3$ (1.5 g, 15 mmol) in MeOH (50 cm$^3$) yielded a dark green solution, that was stirred at room temperature for 3 days. The mixture was evaporated to dryness, and the residues dissolved in the

**Table 1** Experimental details for the single crystal structure determinations in this study.

| | **1**$\cdot$1/2$H_2O\cdot 2CHCl_3$ | **2**$\cdot$1/2$C_5H_{12}$ | **3**$\cdot$3/4$CH_2Cl_2\cdot Hpz^{PhF}$ | **4** |
|---|---|---|---|---|
| Molecular formula | $C_{34}H_{27}Cl_6Cu_2N_{12}O_{0.5}$ | $C_{74.50}H_{62}Cu_4N_{16}$ | $C_{84}H_{61.25}Cl_{1.5}Cu_4F_{12.25}N_{18.50}$ | $C_{36}H_{26}CuF_4N_8$ |
| $M_r$ | 951.46 | 1435.56 | 1869.85 | 710.19 |
| Crystal class | Orthorhombic | Monoclinic | Triclinic | Orthorhombic |
| Space group | *Pbca* | $P2_1/n$ | $P\bar{1}$ | $Pna2_1$ |
| $a$/Å | 27.6069(3) | 18.978(4) | 17.0552(1) | 36.1535(6) |
| $b$/Å | 17.8695(2) | 17.233(3) | 20.9288(1) | 7.69370(10) |
| $c$/Å | 32.0957(4) | 22.798(5) | 25.8492(2) | 10.9951(2) |
| $\alpha$/° | — | — | 90.5532(2) | — |
| $\beta$/° | — | 114.117(8) | 103.5682(3) | — |
| $\gamma$/° | — | — | 106.7792(4) | — |
| $V$/Å$^3$ | 15833.5(3) | 6805(2) | 8557.65(9) | 3058.33(9) |
| $Z$ | 16 | 4 | 4 | 4 |
| $\mu$(Mo-K$\alpha$)/mm$^{-1}$ | 1.525 | 1.289 | 1.109 | 0.781 |
| $T$/K | 150(2) | 100(2) | 150(2) | 150(2) |
| Measured reflections | 82877 | 166799 | 171105 | 21870 |
| Independent reflections | 18006 | 18446 | 39023 | 6837 |
| $R_{int}$ | 0.095 | 0.054 | 0.095 | 0.108 |
| $R(F)^a$ | 0.057 | 0.043 | 0.063 | 0.059 |
| $wR(F^2)^b$ | 0.164 | 0.119 | 0.199 | 0.162 |
| Goodness of fit | 1.039 | 1.008 | 1.058 | 1.042 |
| Flack parameter | — | — | — | 0.043(16) |

$^a$ $R = \Sigma[F_o| - |F_c|]/\Sigma|F_o|$. $^b$ $wR = [\Sigma w(F_o^2 - F_c^2)/\Sigma wF_o^4]^{1/2}$.

minimum volume of $CH_2Cl_2$. Layering the filtered solution with a five-fold excess of hexanes resulted in the formation of blue–green crystals over a period of 2 weeks. These were collected, washed with pentane and dried *in vacuo.* Yield 0.28 g, 30%. Found C, 55.1; H, 3.4; N, 14.3%. Calcd for $C_{81}H_{58}Cu_4F_{12}N_{18}$ C, 55.1; H, 3.3; N, 14.3%. FD mass spectrum ($CHCl_3$): $m/z$ 1827 $[^{63}Cu_5F_3(Pz^{PhF})_3(HPz^{PhF})_6]^+$, 1766 $[^{63}Cu_4F_3(Pz^{PhF})(HPz^{PhF})_7]^+$, 1764 $[^{63}Cu_4F_3(Pz^{PhF})_3(HPz^{PhF})_6]^+$, 1654 $[^{63}Cu_4F_6(Pz^{PhF})_8]^+$, 1218 $[^{63}Cu_4(pz^{PhF})_6]^+$, 1155 $[^{63}Cu_3(pz^{PhF})_6]^+$, 994 $[^{63}Cu_3(pz^{PhF})_5]^+$, 833 $[^{63}Cu_3(pz^{PhF})_4]^+$, 672 $[^{63}Cu_3(pz^{PhF})_3]^+$, 202 $[^{63}CuF(pz^{PhF})_2]^{2+}$, 162 $[Hpz^{PhF}]^+$. ES mass spectrum (MeCN): $m/z$ 490 $[^{63}Cu_2(pz^{PhF})(Hpz^{PhF})(CH_3CN)]^+$, 386 $[^{63}Cu(pz^{PhF})(Hpz^{PhF})]^+$, 301 $[^{63}Cu(pz^{PhF})(CH_3CN)(H_2O)_2]^+$, 265 $[^{63}Cu(pz^{PhF})(CH_3CN)]^+$, 163 $[H_2pz^{PhF}]^+$.

### Synthesis of $[Cu(pz^{PhF})_2(Hpz^{PhF})_2]$ (4)

A solution of $Cu(OH)_2$ (0.20 g, 2.1 mmol) and $Hpz^{PhF}$ (0.68 g, 4.2 mmol) in MeOH (50 cm$^3$) was refluxed for 3 days. The mixture was cooled, filtered and evaporated to dryness, and the turquoise residues redissolved in the minimum volume of $CH_2Cl_2$. Slow diffusion of $Et_2O$ vapour into the filtered solution yielded dark blue crystals which were collected, washed with pentane and dried *in vacuo.* Yield 0.20 g, 13%. Found C, 61.0; H, 3.4; N, 15.8%. Calcd for $C_{36}H_{26}CuF_4N_8$ C, 60.9; H, 3.7; N, 15.8%. ES mass spectrum (MeCN): $m/z$ 386 $[^{63}Cu(pz^{PhF})(Hpz^{PhF})]^+$, 364 $[^{63}Cu_2(pz^{PhF})(CH_3CN)(H_2O)_2]^+$, 301 $[^{63}Cu(pz^{PhF})(CH_3CN)(H_2O)_2]^+$, 265 $[^{63}Cu(pz^{PhF})(CH_3CN)]^+$, 242 $[^{63}Cu(pz^{PhF})(H_2O)]^+$, 163 $[H_2pz^{PhF}]^+$.

### Single crystal X-ray structure determinations

Diffraction data for **2**$\cdot$1/2$C_5H_{12}$ were measured using a Bruker X8 Apex diffractometer, with graphite-monochromated Mo-K$\alpha$ radiation ($\lambda$ = 0.71073 Å) generated by a rotating anode. The other three structure determinations were carried out on a Nonius KappaCCD area detector diffractometer, using graphite-monochromated Mo-K$\alpha$ radiation from a sealed tube source. Both diffractometers were fitted with an Oxford Cryostream low temperature device. Experimental details of the structure determinations in this study are given in Table 1. All the structures were solved by direct methods (*SHELXS96*[38]), and developed by full least-squares refinement on $F^2$ (*SHELXL96*[39]). Figures were produced using *XSEED*,[40] which incorporates *POVRAY*.[41] More information about the crystal structure of **4** is given in the ESI.‡

CCDC reference numbers 632224–632227.

For crystallographic data in CIF or other electronic format see DOI: 10.1039/b618780c

### Single crystal X-ray structure of 1$\cdot$1/2$H_2O\cdot 2CHCl_3$

The asymmetric unit contains two molecules of the complex compound (labelled 'A' and 'B'), four molecules of chloroform and one molecule of water. The final model contains no disorder; although solvent molecule C(59)–Cl(62) exhibits some slightly high thermal parameters, attempts to resolve a second partial solvent molecule in this site were unsuccessful. All non-H atoms were refined anisotropically, and all C-bound H atoms were placed in calculated positions and refined using a riding model. The H atoms in the water molecule O(63) were located in the Fourier map and allowed to refine freely with a common isotropic thermal parameter, subject to the restraints O–H = 0.85(1) Å and H $\cdots$ H = 1.39(2) Å. The highest residual Fourier peak of +1.0 $e$ Å$^{-3}$ lies within the solvent molecule C(55)–Cl(58).

### Single crystal X-ray structure of 2$\cdot$1/2$C_5H_{12}$

The asymmetric unit of the crystal contains one complex molecule lying on a general position, and a disordered region of solvent about the crystallographic inversion centre $1-x$, $1-y$, $-z$. The phenylpyrazolido ligands N(5)–C(15) and N(82)–C(92) are disordered, each over three equally occupied orientations. The phenyl group C(76)–C(81) is also disordered over two sites with refined occupancies of 0.55 and 0.45. The following restraints were applied to these disordered groups: phenyl C–C = 1.39(2), phenyl 1,3-C · · · C = 2.41(1), C{pyrazole}–C{phenyl} = 1.46(1), N–N = 1.34(1), pyrazole C–N = 1.34(1), pyrazole C=N = 1.35(1), pyrazole C–C = 1.37(1) and pyrazole C=C = 1.39(1) Å. Two partial pentane solvent orientations were refined, each with occupancy 0.25 and sharing one common C atom. The C–C bonds in the disordered solvent were restrained to 1.54(1) Å, and 1,3-C · · · C distances to 2.51(1) Å. All non-H atoms with occupancies >0.50 were refined anisotropically, while all H atoms were placed in calculated positions and refined using a riding model.

### Single crystal X-ray structure of $3{\cdot}3/4CH_2Cl_2{\cdot}HPz^{PhF}$

The asymmetric unit contains two molecules of the complex, labelled 'A' and 'B'. Where required, partial disorder sites of atoms in molecule 'A' are given the label 'C', and those in molecule 'B' are labelled as 'D'. The asymmetric unit also contains four weakly occupied dichloromethane environments C(1S)–Cl(3S) (fully occupied), C(4S)–Cl(6S) (occupancy 0.2), C(7S)–Cl(9S) (0.1) and C(10S)–Cl(12S) (0.2); and, two weakly occupied 3{5}-(4-fluorophenyl)pyrazole sites N(1E)–F(12E) (occupancy 0.3) and N(13E)–F(24E) (0.2). Partial molecules N(1E)–F(12E), N(13E)–F(24E) and C(10S)–Cl(12S) occupy the same region of space in the lattice, so these sites cannot be simultaneously occupied. The same is true of C(4S)–Cl(6S), C(7S)–Cl(9S) and partial ligand [N(11B), N(12B), C(51B)–F(60B)].

The two complex molecules show extensive, and similar, patterns of disorder. The following 4-fluorophenyl substituents are disordered, each over two equally occupied sites: C(34A/C)–F(40A/C), C(44A/C)–F(50A/C)], C(74A/C)–F80(A/C), C(44B/D)–F(50B/D) and C(74B/D)–F(80B/D). The following 5-(4-fluorophenyl)pyrazole ligands are also disordered, each over two equally occupied sites: [N(13A/C), N(14A/C), C(61A/C)–F(70A/C)], [N(11B/D), N(12B/D), C(51B/D)–F(60B/D]) and [N(13B/D), N(14B/D), C(61B/D)–F(70B/D)]. The following restraints were applied to the disordered groups and weakly occupied pyrazole and solvent sites in the model: intra-pyrazole N–N = 1.34(1) Å, intra-pyrazole N–C = 1.35(1) Å, intra-pyrazole N=C = 1.34(1) Å, intra-pyrazole C–C = 1.39(1) Å, intra-pyrazole C=C = 1.37(1) Å, C–F = 1.33(1) Å, C=Cl = 1.78(2) Å, Cl · · · Cl = 2.91(2) Å and all disordered or partially occupied $C_6H_4$ groups were refined as rigid hexagons. All atoms with occupancy ≤0.5 were refined anisotropically, and all H atoms were placed in calculated positions and refined using a riding model. There is one residual Fourier hole of −1.3 *e* $Å^{-3}$, 0.8 Å from Cu(2A).

### Single crystal X-ray structure of 4

No disorder was detected during refinement, and no restraints were applied. All non-H atoms were refined anisotropically, while all H atoms were placed in calculated positions and refined using a riding model. The protonated and deprotonated N atoms of each hydrogen-bonded pair were distinguished in two ways. First, because appropriately positioned residual Fourier peaks were present in the vicinity of N(3) and N(27), but not N(15) and N(39). Second, because the Cu–N bonds to the protonated pyrazole N atoms N(2) and N(26) are 6 sus longer than those to the deprotonated pyrazolido ligand donors N(14) and N(38). The deepest residual Fourier hole of −1.0 *e.* $Å^{-3}$ is 0.9 Å from Cu(1).

### Other measurements

Electrospray (ES) mass spectra were performed with a Micromass LCT TOF spectrometer using a MeCN feed solution, while field desorption (FD) mass spectra employed a Waters GCT premiere spectrometer and were taken from chloroform solutions. All peaks show correct isotopic distributions for their assigned molecular ions. Mass peaks labelled as mixtures of monomeric and dimeric species show $(m/z) : (m/z) + 2$ isotope ratios midway between that predicted for a mono-copper (0.44) and dicopper (0.89) species. CHN microanalyses were performed by the University of Leeds School of Chemistry microanalytical service. Variable temperature magnetic susceptibility measurements were obtained in the solid state using a Quantum Design SQUID magnetometer operating at 1000 G. Diamagnetic corrections for the sample (from Pascal's constants[18]) and the sample holder were applied to the data. Theoretical fits of the susceptibility data were carried out using *SIGMAPLOT*.[42] *X*-band EPR spectra were obtained using a Bruker EMX spectrometer fitted with an ER4119HS resonator and ER4131VT cryostat. *W*-band spectra were recorded using a commercial Bruker *ELEXSYS* spectrometer operating at 94 GHz frequency at 0–6 T field range. The temperature was stabilised by an Oxford Instrumets ITC503 auto-tuning temperature controller at ±1 K precision. EPR spectra were analysed and simulated using *XSophie* commercial software.

## Acknowledgements

The authors would like to thank Dr H. J. Blythe (University of Sheffield) for help with the magnetic measurements, and the EPSRC and the Leverhulme Trust for funding.

## References

1 G. La Monica and G. A. Ardizzoia, *Prog. Inorg. Chem.*, 1997, **46**, 151 and references therein.

2 A. P. Sadimenko and S. S. Basson, *Coord. Chem. Rev.*, 1996, **147**, 247; L. A. Oro, M. A. Ciriano and C. Tejel, *Pure Appl. Chem.*, 1998, **70**, 779.

3 G. Mezei, P. Baran and R. G. Raptis, *Angew. Chem., Int. Ed.*, 2004, **43**, 574.

4 See *e.g.*: R. G. Raptis, I. P. Georgakaki and D. C. R. Hockless, *Angew. Chem., Int. Ed.*, 1999, **38**, 1632; D. T. Puerta and S. M. Cohen, *Chem. Commun.*, 2003, 1278; G. Mezei, M. Rivera-Carrillo, R. G. Raptis and S. Tanase, *Inorg. Chim. Acta*, 2004, **357**, 3721; G. Aromi, E. Bouwman, H. Kooijman, A. L. Spek and J. Reedijk, *Chem. Commun.*, 2005, 3147; V. Chandrasekhar, L. Nagarajan, K. Gopal, V. Baskar and P. Kogerler, *Dalton Trans.*, 2005, 3143.

5 X. Liu, C. A. Kilner and M. A. Halcrow, *Chem. Commun.*, 2002, 704; S. L. Renard, C. A. Kilner, J. Fisher and M. A. Halcrow, *J. Chem. Soc., Dalton Trans.*, 2002, 4206; S. L. Renard, A. Franken, C. A. Kilner, J. D. Kennedy and M. A. Halcrow, *New J. Chem.*, 2002, **26**, 1634; S. L. Renard, I. Sylvestre, S. A. Barrett, C. A. Kilner and M. A. Halcrow, *Inorg. Chem.*, 2006, **45**, 8711.

6 S. Nieto, J. Pérez, V. Riera, D. Miguel and C. Alvarez, *Chem. Commun.*, 2005, 546; S. Nieto, J. Pérez, L. Riera, V. Riera and D. Miguel, *Chem.–Eur. J.*, 2006, **12**, 2244; M. Arroyo, D. Miguel, F. Villafane, S. Nieto, J. Pérez and L. Riera, *Inorg. Chem.*, 2006, **45**, 7018.

7 A. Looney, G. Parkin and A. L. Rheingold, *Inorg. Chem.*, 1991, **30**, 3099; D. L. Reger, Y. Ding, A. L. Rheingold and R. L. Ostrander, *Inorg. Chem.*, 1994, **33**, 4226; M. Onishi, M. Yamaguchi, S. Kumagae, H. Kawano and Y. Arikawa, *Inorg. Chim. Acta*, 2006, **359**, 990.

8 C. M. Pask, K. D. Camm, N. J. Bullen, M. J. Carr, W. Clegg, C. A. Kilner and M. A. Halcrow, *Dalton Trans.*, 2006, 662; L. F. Jones, K. D.

Camm, C. A. Kilner and M. A. Halcrow, *CrystEngComm*, 2006, **8**, 719.
9 X. Liu, J. A. McAllister, M. P. de Miranda, B. J. Whitaker, C. A. Kilner and M. A. Halcrow, *Angew. Chem., Int. Ed.*, 2002, **41**, 756.
10 X. Liu, A. C. McLaughlin, M. P. de Miranda, E. J. L. McInnes, C. A. Kilner and M. A. Halcrow, *Chem. Commun.*, 2002, 2978.
11 X. Liu, J. A. McAllister, M. P. de Miranda, E. J. L. McInnes, C. A. Kilner and M. A. Halcrow, *Chem.–Eur. J.*, 2004, **10**, 1827.
12 X. Liu, M. P. de Miranda, E. J. L. McInnes, C. A. Kilner and M. A. Halcrow, *Dalton Trans.*, 2004, 59.
13 M. K. Ehlert, S. J. Rettig, A. Storr, R. C. Thompson and J. Trotter, *Can. J. Chem.*, 1989, **67**, 1970; M. K. Ehlert, S. J. Rettig, A. Storr, R. C. Thompson and J. Trotter, *Can. J. Chem.*, 1991, **69**, 432; M. K. Ehlert, A. Storr, R. C. Thompson, F. W. B. Einstein and R. J. Batchelor, *Can. J. Chem.*, 1993, **71**, 331; A. Cingolani, S. Galli, N. Masciocchi, L. Pandolfo, C. Pettinari and A. Sironi, *J. Am. Chem. Soc.*, 2005, **127**, 6144.
14 A. J. Amoroso, A. M. Cargill Thompson, J. C. Jeffery, P. L. Jones, J. A. McCleverty and M. D. Ward, *J. Chem. Soc., Chem. Commun.*, 1994, 2751.
15 S. Trofimenko, J. C. Calabrese and J. S. Thompson, *Inorg. Chem.*, 1987, **26**, 1507.
16 M. A. Halcrow, E. J. L. McInnes, F. E. Mabbs, I. J. Scowen, M. McPartlin, H. R. Powell and J. E. Davies, *J. Chem. Soc., Dalton Trans.*, 1997, 4025.
17 A. W. Addison, T. N. Rao, J. Reedijk, J. van Rijn and G. C. Verschoor, *J. Chem. Soc., Dalton Trans.*, 1984, 1349.
18 C. J. O'Connor, *Prog. Inorg. Chem.*, 1982, **29**, 203.
19 G. V. Rubenacker, J. E. Drumheller, K. Emerson and R. D. Willett, *J. Magn. Magn. Mater.*, 1986, **54–57**, 1483.
20 T.-L. Hu, J.-R. Li, C.-S. Liu, X.-S. Shi, J.-N. Zhou, X.-H. Bu and J. Ribas, *Inorg. Chem.*, 2006, **45**, 162.
21 See *e.g.*: T. Kamiusuki, H. Ōkawa, N. Matsumoto and S. Kida, *J. Chem. Soc., Dalton Trans.*, 1990, 195; C. Miranda, F. Escartí, L. Lamarque, E. García-España, P. Navarro, J. Latorre, F. Lloret, H. R. Jiménez and M. J. R. Yunta, *Eur. J. Inorg. Chem.*, 2005, 189; J. Teichgräber, G. Leibeling, S. Dechert and F. Meyer, *Z. Anorg. Allg. Chem.*, 2005, **631**, 2613.
22 V. P. Hanot, R. D. Toussaint, J. Kolnaar, J. G. Haasnoot, J. Reedijk, H. Kooijiman and A. L. Spek, *J. Chem. Soc., Dalton Trans.*, 1996, 4275; H. Matsushima, H. Hamada, K. Watanabe, M. Koikawa and T. Tokii, *J. Chem. Soc., Dalton Trans.*, 1999, 971.
23 See *e.g.*: H. Zhang, D. Fu, F. Ji, G. Wang, K. Yu and T. Yao, *J. Chem. Soc., Dalton Trans.*, 1996, 3799; E. Spodine, A. M. Atria, J. Valenzuela, J. Jalocha, J. Manzur, A. M. García, M. T. Garland, O. Peña and J.-Y. Saillard, *J. Chem. Soc., Dalton Trans.*, 1999, 3029; M. F. Isklander, T. E. Khalil, W. Haase, R. Werner, I. Svoboda and H. Fuess, *Polyhedron*, 2001, **20**, 2787; A. F. Stassen, W. L. Driessen, J. G. Haasnoot and J. Reedijk, *Inorg. Chim. Acta*, 2003, **350**, 25.
24 K. L. V. Mann, E. Psillakis, J. C. Jeffery, L. H. Rees, N. M. Harden, J. A. McCleverty, M. D. Ward, D. Gatteschi, F. Totti, F. E. Mabbs, E. J. L. McInnes, P. C. Riedi and G. M. Smith, *J. Chem. Soc., Dalton Trans.*, 1999, 339.
25 K. Singh, J. R. Long and P. Stavropoulos, *Inorg. Chem.*, 1998, **37**, 1073.
26 D. Ajo, A. Bencini and F. Mani, *Inorg. Chem.*, 1988, **27**, 2437.
27 N. Masciocchi, G. A. Ardizzoia, A. Maspero, G. LaMonica and A. Sironi, *Inorg. Chem.*, 1999, **38**, 3657; N. Masciocchi, G. A. Ardizzoia, S. Brenna, G. La Monica, A. Maspero, S. Galli and A. Sironi, *Inorg. Chem.*, 2002, **41**, 6080; A. Cingolani, S. Galli, N. Masciocchi, L. Pandolfo, C. Pettinari and A. Sironi, *Dalton Trans.*, 2006, 2479.
28 P. Baran, C. M. Marrero, S. Perez and R. G. Raptis, *Chem. Commun.*, 2002, 1012.
29 K. Umakoshi, Y. Yamauchi, K. Nakamiya, T. Kojima, M. Yamasaki, H. Kawano and M. Onishi, *Inorg. Chem.*, 2003, **42**, 3907 and 6584 (erratum).
30 W. Burger and J. Strähle, *Z. Anorg. Allg. Chem.*, 1985, **529**, 111.
31 G. A. Ardizzoia, G. La Monica, S. Cenini, M. Moret and N. Masciocchi, *J. Chem. Soc., Dalton Trans.*, 1996, 1351; N. Masciocchi, G. A. Ardizzoia, G. La Monica, M. Moret and A. Sironi, *Inorg. Chem.*, 1997, **36**, 449.
32 W. Burger and J. Strähle, *Z. Anorg. Allg. Chem.*, 1986, **539**, 27.
33 N. Buchholz and R. Mattes, *Angew. Chem., Int. Ed. Engl.*, 1986, **25**, 1104.
34 D. L. Thorn, R. L. Harlow and N. Herron, *Inorg. Chem.*, 1995, **34**, 2629; D. Riou, F. Taulelle and G. Ferey, *Inorg. Chem.*, 1996, **35**, 6392.
35 F.-Q. Liu, D. Stalke and H. W. Roesky, *Angew. Chem., Int. Ed. Engl.*, 1995, **34**, 1872.
36 B. Werner, T. Kraüter and B. Neumüller, *Inorg. Chem.*, 1996, **35**, 2977; B. Werner and B. Neümuller, *Chem. Ber.*, 1996, **129**, 355; Y. Yang, J. Pinkas, M. Schäfer and H. W. Roesky, *Angew. Chem., Int. Ed.*, 1998, **37**, 2650.
37 P. L. Watson, T. H. Tulip and I. Williams, *Organometallics*, 1990, **9**, 1999.
38 G. M. Sheldrick, *Acta Crystallogr., Sect. A*, 1990, **A46**, 467.
39 G. M. Sheldrick, *SHELXL97, Program for the refinement of crystal structures*, University of Göttingen, Germany, 1997.
40 L. J. Barbour, *J. Supramol. Chem.*, 2003, **1**, 189.
41 *POVRAY v. 3.5*, Persistence of Vision Raytracer Pty. Ltd., Williamstown, Victoria, Australia, 2002, http://www.povray.org.
42 *SIGMAPLOT*, v. 8.02, SPSS Scientific Inc., Chicago IL, 2002.